

Direct observation of the critical state field profile in a $\text{YBa}_2\text{Cu}_3\text{O}_{7-y}$ single crystal

T. Tamegai,* L. Krusin-Elbaum, L. Civale, P. Santhanam, M. J. Brady, W. T. Masselink, F. Holtzberg, and C. Feild

IBM Thomas J. Watson Research Center, P.O. Box 218, Yorktown Heights, New York 10598

(Received 4 November 1991)

We report direct imaging of the critical state in a $\text{YBa}_2\text{Cu}_3\text{O}_{7-y}$ single crystal. The self-field profiles are obtained by mechanically scanning a high-spatial-resolution Hall-probe array above the crystal surface. The measured field distributions confirm Bean's assumption of homogeneity, setting the relevant length scale for the evaluation of the critical currents as the sample size, and are a proof against the weak-link behavior in such crystals.

A reliable determination of the critical currents in single crystals of high-temperature superconductors is undoubtedly vital to the understanding of pinning of magnetic vortices in these materials and consequently to their important future applications. The measurements of magnetic hysteresis, M vs H , is a particularly convenient noncontact way to probe the behavior of critical currents in small and delicate crystals, where it avoids many serious problems in electrically contacting them through surface oxide layers.¹ But to extract the information about the critical current densities J_c one pays the price of a complex analysis² and a reliance on a model relating magnetization to J_c . The accepted phenomenology is that of the critical-state model describing the way in which J_c is limited by the Lorentz force, which even in the simplest form proposed by Bean³ explains many features of the high-field magnetic hysteresis loops.¹ There are numerous extensions of the original Bean work which include H_{c1} ,^{4,5} surface barriers,^{5,6} and various forms of $J_c(H)$ dependence.⁴ However, in all of them an important assumption is the *homogeneity* of the superconductor with defects, which sets the relevant length scale to be the size of the crystal. The basic premise of the model is that above H_{c1} in the presence of pinning the vortices are organized so that the locally averaged magnetic induction B inside a slab of the superconductor forms a gradient according to a modified Ampère's law⁷ $dB/dx = (4\pi/c)J_c$. Here, J_c is a screening current density flowing to a depth necessary to reduce the field to H_{c1} ; below H_{c1} there is a complete screening. Above H_{c1} , the width of the magnetic hysteresis ΔM can be used to derive J_c values. For instance, in a slab geometry of thickness d and field applied along the plane of the slab, a simple relation $J_c \approx 40\Delta M/d$ (Refs. 1 and 3) follows. This widely used formula would not hold if the material is better described in terms of isolated grains with only weak coupling between the grains—then the relevant length scale is set by the grain size.⁸

Clearly, it is important to test the validity of the Bean description in single crystals of oxide superconductors, where arguments were made for the existence of some kind of granularity,⁹ raising doubts as to the estimates of the critical currents and the general understanding of flux pinning. The most convincing proof against granularity would be the observation of the locally averaged magnetic induction profile which is almost triangular or "sandpile"

like.³ In contrast, the collection of grains will produce a different spatial image of the local induction; a "flat-top-like" profile, which should be easily distinguished in the experiment.

In this paper, we report a *direct* observation of the critical state field profile in a $\text{YBa}_2\text{Cu}_3\text{O}_{7-y}$ single crystal¹⁰ which we find to be consistent with the Bean model with the specific features peculiar to the thin-plate geometry typical of high- T_c single crystals. We probe the field distribution by measuring the local magnetic fields near the crystal surface by a photolithographically patterned linear array of Hall probes, which is mechanically scanned in the direction orthogonal to the array. The Hall-probe technique for imaging the critical state has been used on a conventional superconductor Nb-Ti,¹¹ and recently there have been reports of measuring the local fields in high- T_c materials^{12,13} as well. Our technique allows high-spatial-resolution recording of the local-field distributions simultaneously across several paths on the crystal and thus allows for correlation of geometry related features, such as edge effects.

The Hall-probe arrays are fabricated using silicon-doped GaAs epitaxial film (1500 \AA , $n = 10^{18} \text{ cm}^{-3}$). The particular array used in this experiment consists of seven Hall probes, each composed of a cross geometry of two $10\text{-}\mu\text{m}$ -wide wires, having a sensitivity of about 70 V/A T . The integrating area of each probe is $\approx 10 \times 10 \mu\text{m}^2$, and the typical dimension being scanned is about 1 mm . The single crystal of $\text{YBa}_2\text{Cu}_3\text{O}_{7-y}$ with dimensions $881 \times 562 \times 23 \mu\text{m}^3$ (c axis is parallel to the shortest dimension) is glued to a stage which is moved horizontally in a vertical field generated by a superconducting solenoid as indicated schematically in Fig. 1. The motion is accomplished by means of a micrometer screw with a tapered lower end, powered by a computer-controlled stepping motor. This device has a reproducibility of about $10 \mu\text{m}$, limited by the mechanical imperfections of the tapered end. The calibration of the travel distance in terms of the rotation angle of the micrometer screw is performed at room temperature and such calibration is in good agreement with the self-calibrating nature of the measurement itself; i.e., the size of the crystal is apparent in the imaged field profile. We used five probes for this experiment, four of which labeled P2 through P5, were spaced 200 or 300 μm apart as shown in Figs. 1(b) and 1(c). A separate probe (P1) positioned 3 mm away from the others on the

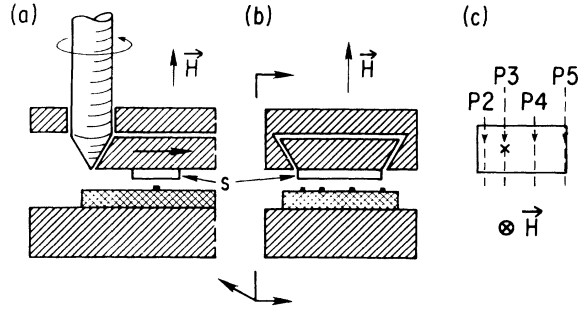


FIG. 1. Schematic drawing of the mechanical device used for scanning the Hall probe array. (a) The micrometer screw and the sample (S) stage. (b) The side view of the sample stage and Hall probe chip with the positions of the measuring probes indicated as protrusions. (c) Top view on the crystal; the dashed lines indicate where on the crystal the local field profiles were recorded. The cross indicates the location at which the local hysteresis loop of Fig. 2(a) was measured.

same chip was used for field calibration. The distance from the crystal to the array was set for this measurement to $\approx 100 \mu\text{m}$ (the details of the Hall-probe design and the scanning mechanism will be published elsewhere). The magnetic field was applied along the c axis and the component of the local field parallel to the applied field near the sample surface was measured by passing a current of $40 \mu\text{A}$ through the probes.

First, we relate our local measurement to the more standard superconducting quantum interference device (SQUID) or vibrating-sample magnetometer studies. Our Hall probes are sensitive to the vertical component of the local field $\mathbf{B}(\mathbf{r})$. By subtracting the applied field \mathbf{H} , we obtain the z component of $\mathbf{H}_l(\mathbf{r}) = \mathbf{B}(\mathbf{r}) - \mathbf{H}$, which is the self-field generated by the current flowing in the crystal:

$$\mathbf{H}_l(\mathbf{r}) = \frac{1}{c} \int_V d^3r' \frac{\mathbf{J}(\mathbf{r}') \times (\mathbf{r} - \mathbf{r}')}{|\mathbf{r} - \mathbf{r}'|^3}, \quad (1)$$

where V is the volume of the sample in which the currents are flowing. The Bean model imposes $|\mathbf{J}(\mathbf{r}')| = J_c$, thus H_l equals J_c times a geometric coefficient. We measure H_{lz} close to the sample surface. At distances that are large compared with the sample size, the dipolar term in a multipolar expansion of Eq. (1) dominates, $\mathbf{H}_l(\mathbf{r}) \approx \nabla \times [(\mathbf{m} \times \mathbf{r})/r^3]$, where $\mathbf{m} = (1/2c) \int_V d^3r' [\mathbf{r}' \times \mathbf{J}(\mathbf{r}')]$. This total magnetic moment, which is also proportional to J_c , is the quantity measured in SQUID and vibrating-sample magnetometers. So, if the Bean model holds, H_{lz} and m ($=MV$) are proportional. To verify this relation experimentally, we position the array about the center of the crystal roughly as indicated in Fig. 1(c). Figure 2(a) shows the local hysteresis loop H_{lz} vs H measured by the probe P3 at $T = 10 \text{ K}$ up to a field of 80 kOe . Figure 2(b) shows the integrated measurement of m vs H loop on the same crystal also at $T = 10 \text{ K}$ with the SQUID magnetometer up to the maximum available field of 55 kOe . The two loops are obviously very similar; the structure at low fields, which is somewhat different in both cases, is a

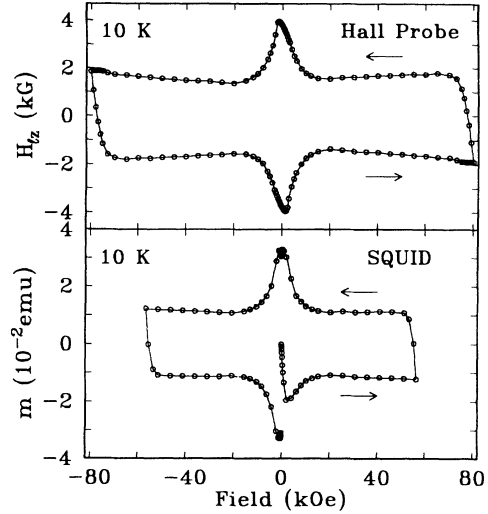


FIG. 2. Magnetic hysteresis measured at $T = 10 \text{ K}$ by (a) Hall probe P3 near the center of the crystal and (b) measured by a SQUID on the same crystal.

consequence of finite H_{c1} and is discussed in detail elsewhere.¹⁴ Thus we take H_{lz} to be proportional to J_c .

We now scan the probes to measure the self-field distribution $H_{lz}(x)$. To prepare the crystal in the critical state, we first sweep H up to 80 kOe at a fixed temperature. The field is then decreased and stabilized at some lower value for the measurement. This means that we are sitting on the decreasing branch of the hysteresis loop. To avoid a large initial magnetic relaxation, the scan is delayed by 30 min after establishing the critical state. Profiles of $H_{lz}(x)$ at 10 K and various external fields taken with P3 are shown in Fig. 3. We note the almost triangular Bean-like field profiles for the range of external fields from 0 to 70 kOe ; the gradient of H_{lz} at different fields gives, of course,

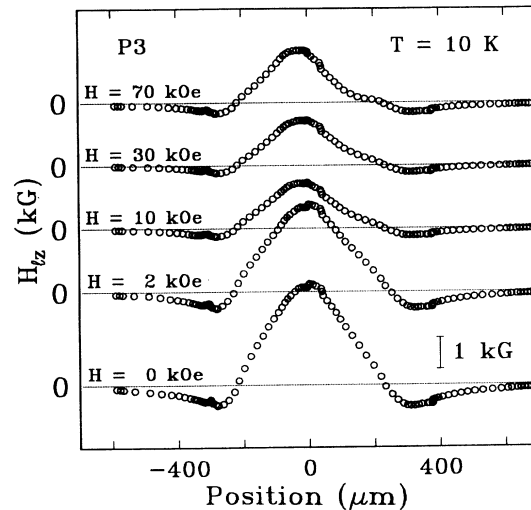


FIG. 3. Local self-field profiles at 10 K imaged near the center of the crystal (probe P3) for several values of the applied field.

the field dependence of J_c . A distinct feature of these profiles is that right at the edge of the crystal the imaged self-field is negative. This is also clearly seen in Fig. 4, which shows the self-field profiles measured by scanning probes P2-P5 at $T=10$ K and zero external field. The field reversal at the edges is apparent in the field profiles measured across different paths. Images recorded by P3 and P4 near the center of the crystal are very similar. Probe P2, which records the self-field closer to the edge but still over the crystal, shows a diminished profile. And the profile imaged by P5, right at the edge of the crystal, is completely reversed. The field reversal at the edges of the crystal will be discussed later.

These Bean-like field distributions over the entire width of the crystal are *direct proof* against granularity. A small scale granularity at high fields and temperatures was suggested by Daeumling, Seuntjens, and Larbalestier.⁹ They argue that even small oxygen deficiencies contribute significantly to the weak-link properties of the single crystals of $YBa_2Cu_3O_{7-y}$, resulting in an anomalous magnetization. Yeshurun *et al.*¹⁵ tried to resolve this issue by using a laser ablation technique to grid pattern the thin $YBa_2Cu_3O_{7-y}$ and $BiSrCaCuO$ crystals to test the scaling of J_c with the size of the grid. Their results are inconsistent with the granularity on such a small scale but suggest the presence of some larger scale defects impeding current flow; they find a sublinear size dependence of J_c for grid size greater than $200 \mu\text{m}$. In our direct imaging technique, the existence of weak links would produce "triangular" field profiles on the scale of the grain diameter. The large scale image of the local field right at the crystal surface would be sawtooth like and irregular. At some distance t away from the surface, the variations will be smoothed out to an essentially flat distribution with a ripple which depends on t . Thus we can say with reasonable confidence that in the field and temperature range of this

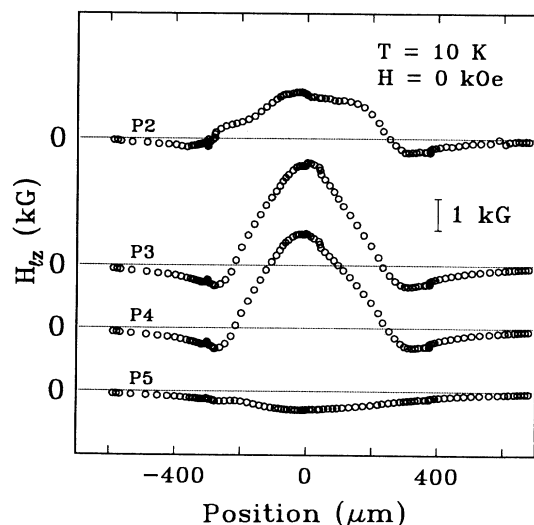


FIG. 4. Local self-field profiles at 10 K imaged across four different paths on the crystal as indicated in Fig. 1(c). The field reversal near the edges and a fully negative field profile at probe P5 are explained by the field divergencies inherent in the plate-like geometry of the crystal (see text and Fig. 5).

study, $YBa_2Cu_3O_{7-y}$ crystals are not granular on any scale and homogeneous on the scale of at least $10 \mu\text{m}$, which is our spatial resolution. It could still be argued that the crystal is composed of "grains" which are so strongly coupled through Josephson junctions (JJ), that the J_c we are measuring is in reality the critical current of the JJ array and the true bulk J_c is much higher. Of course, the critical state field profile would be indistinguishable then from that expected for a uniform bulk material. If that were the case, however, a decoupling of grains should be observed at high enough fields. We find no evidence of the decoupling in magnetic fields up to 8 T and thus we conclude that the description in terms of such JJ arrays is not supported by the experimental data.

Now we discuss the feature of the observed H_{zz} profile which is not predicted in the original Bean derivation³ for the geometry of an infinite cylinder or a slab with the external field parallel to the slab;¹⁶ i.e., the negative field at the edges before the recovery to the zero self-field value farther away from the crystal. The effects of geometry in thin superconductors, with external field applied along the thin direction, were extensively discussed in the literature.¹⁷⁻¹⁹ Daeumling and Larbalestier¹⁸ performed numerical calculations on a thin disk and showed that for a uniform bulk circumferential current density J_c , the vortex lines within the superconductor become severely curved and the vertical component of the field reverses at the edges, although the conventional Bean linear scaling of the magnetization with the disk radius R remains unchanged. Conner and co-workers¹⁹ extended this work with a self-consistent analysis of the current flow in a thin superconducting disk including anisotropy and field

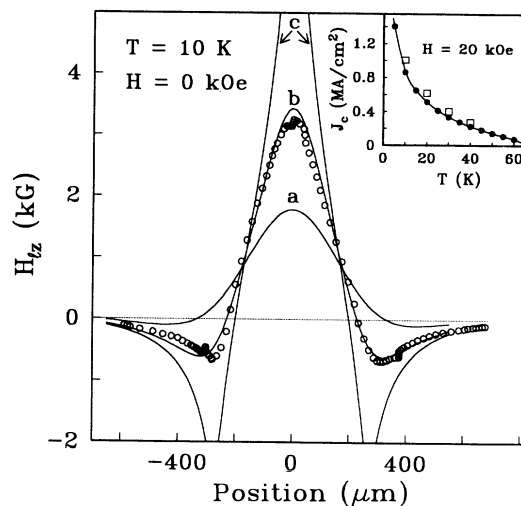


FIG. 5. The self-field profile obtained from scanning near the center of the crystal (probe P3) and calculated field distributions generated by the current in an infinite strip of width w and thickness d ($w/d=100$) measured at (a) $t=25 \mu\text{m}$, (b) $100 \mu\text{m}$ ($\approx 5d$), and (c) $200 \mu\text{m}$ above the strip. The inset shows $J_c(T)$ at $H=20$ kOe derived from the SQUID measurements of m vs H (solid dots) and $J_c(T)$ obtained from the fits to the measured self-field profiles (open squares). J_c of $\sim 10^6$ A/cm² is typical of single crystals at 4.2 K.

dependence of J_c and came to the same conclusion on scaling but with the slope $d(\Delta M)/dR$ below the Bean value.

A more accessible insight comes from a very simple calculation we have done for a thin strip of width w , thickness d , and an infinite length, where in the critical state uniform currents flow in opposite directions in either half of the strip,¹⁴ a situation which well approximates the platelike geometry of our $\text{YBa}_2\text{Cu}_3\text{O}_{7-y}$ crystal when the field is applied along the shortest dimension. At the surface of the strip, the calculated H_{Iz} profile exhibits divergencies at the center and at the edges, where the field at the edges is of the opposite sign. These divergencies are smoothed out in real crystals due to both the field dependence of J_c and a finite distance t separating the Hall-probe array from the crystal. Figure 5 shows the result of such calculation for the self-field profile imaged with the probe P3 at $T=10$ K, $H=0$, and three different distances t . Very close to the crystal surface ($t=25$ μm) the divergencies are apparent. The agreement with data is best with $t=100$ μm , which is roughly the experimentally determined value of t . At larger distances the profile is further diminished. The only fitting parameter in our cal-

ulation is J_c . Since such simple calculation reproduces remarkably well the experimental profiles, performing it for the profiles at various fields and temperatures, and yields values of $J_c(T, H)$ which can be compared with the J_c values obtained from the analysis of the magnetic hysteresis loops measured with SQUID. For example, the inset in Fig. 5 shows $J_c(T)$ for our crystal at 20 kOe determined from both the Hall-probe self-field profiles and the SQUID measurements. In the SQUID technique, J_c was calculated using the sandpile model adequate for a rectangular sample. The agreement on the temperature dependence is remarkably good. The small difference in the absolute value ($\sim 15\%$) is not surprising, given the extreme simplicity of the assumptions in both approaches.

In summary, we have imaged the local self-field profiles in the critical state of $\text{YBa}_2\text{Cu}_3\text{O}_{7-y}$ single crystal by mechanically scanning the Hall-probe array above the crystal surface. We find that Bean's assumption of homogeneity is valid there and that the relevant length scale for the evaluation of the critical currents is the sample size. The shape of H_{Iz} profile is well understood, when one considers a pattern of current flow in a platelike geometry of the sample.

*Present address: Institute for Solid State Physics, University of Tokyo, Roppongi, Minato-ku, Tokyo 106, Japan.

¹A. P. Malozemoff, in *Physical Properties of High Temperature Superconductors I*, edited by D. M. Ginsberg (World Scientific, Singapore, 1989), p. 71.

²A. M. Campbell and J. E. Evetts, *Adv. Phys.* **21**, 199 (1972).

³C. P. Bean, *Rev. Mod. Phys.* **36**, 31 (1964).

⁴P. Chaddah, G. Ravi Kumar, A. K. Grover, C. Radhakrishnamurthy, and G. V. Subba Rao, *Cryogenics* **29**, 907 (1989).

⁵J. R. Clem, *J. Appl. Phys.* **50**, 3518 (1979).

⁶H. A. Ullmaier, *Phys. Status Solidi* **17**, 631 (1966).

⁷For arbitrary geometry one should use the vector Maxwell's equation $\nabla \times \mathbf{B} = (4\pi/c)\mathbf{J}_c$.

⁸L. Civale, H. Safar, F. de la Cruz, D. A. Esparza, and C. A. D'Ovidio, *Solid State Commun.* **65**, 129 (1988).

⁹M. Daeumling, J. M. Seuntjens, and D. C. Larbalestier, *Nature (London)* **346**, 332 (1990).

¹⁰F. Holtzberg and C. Feild, *Eur. J. Solid State Inorg. Chem.* **27**, 107 (1990).

¹¹H. T. Coffey, *Cryogenics* **7**, 73 (1968).

¹²M. Konczykowski, F. Holtzberg, and P. Lejay, *Supercond. Sci. Technol.* **4**, 8337 (1991).

¹³D. A. Brawner, Z. Z. Wang, and N. P. Ong, *Bull. Am. Phys. Soc.* **36** (3), 1064 (1991).

¹⁴T. Tamegai, L. Krusin-Elbaum, P. Santhanam, M. J. Brady, W. T. Masselink, F. Holtzberg, and C. Feild, *Phys. Rev. B* **45**, 2589 (1992).

¹⁵Y. Yeshurun, M. W. McElfresh, A. P. Malozemoff, J. Hagerhorst-Trehwella, J. Mannhart, F. Holtzberg, and G. V. Chandrasekhar, *Phys. Rev. B* **42**, 6332 (1990).

¹⁶The Bean calculation is valid in general for the samples with the translational symmetry along the direction of the external field.

¹⁷D. J. Frankel, *J. Appl. Phys.* **50**, 5402 (1979).

¹⁸M. Daeumling and D. C. Larbalestier, *Phys. Rev. B* **40**, 9350 (1989).

¹⁹L. W. Conner and A. P. Malozemoff, *Phys. Rev. B* **43**, 402 (1991); L. W. Conner, A. P. Malozemof, and I. A. Campbell, *ibid.* **44**, 403 (1991).